N91-21195

MAGNETIC BEARINGS for a SPACEFLIGHT OPTICAL DISK RECORDER

Richard Hockney, Vijay Gondhalekar, Timothy Hawkey

SatCon Technology Corporation

12 Emily Street

Cambridge

MA 02139-4507

Magnetic Bearings for a Spaceflight Optical Disk Recorder

Richard Hockney, Vijay Gondhalekar, Timothy Hawkey

SatCon Technology Corporation
12 Emily Street
Cambridge, MA 02139

Presented at: Workshop on Aerospace Applications of Magnetic Suspension Technology
NASA Langley Research Center, Hampton, VA - September 1990

ABSTRACT

Optical-disk data recording technology is being developed by NASA for space applications. This technology has made possible devices which provide capacities of tens of gigabits, and data-rates of hundreds of megabits-per-second through the use of arrays of solid-state lasers applied to a magneto-optic disk. Bearings are an area where improvements are needed to allow these systems to be utilized in space applications. The porous-graphite air bearings used for the linear translator of the read/write head in the prototype unit, as well as the bearings used in the rotary spindle would be replaced by either magnetic bearings or mechanical (ball or roller) bearings. Based upon past experience, roller or ball bearings are not feasible for the translation stage. Unsatisfactory, although limited, experience exists with ball bearing spindles also. Magnetic bearings are an excellent alternative for both the translational and rotational stages of the devices.

This paper reports on the development and testing of a magnetic bearing system for the translator of the read/write head in a magneto-optic disk drive. The asymmetrical three-pole actuators with permanent-magnet bias support the optical head, and its tracking and focusing servos, through their radial excursion above the disk. The specifications for the magnetic bearing are presented, along with the configuration of the magnetic hardware. Development of a five degree-of-freedom collision model is examined which allowed assessment of the system response during large-scale transients. This model also aided in the establishing the philosophy and strategy for system start-up which are discussed. Finally, experimental findings and the results of performance testing are presented including the roll-off of current-to-force due to eddy-current loss in the magnetic materials.

1. SPECIFICATIONS

Definition of the specifications for the magnetic bearings for the optical disk buffer was facilitated by the decision to make the baseline design capable of retrofit into the existing NASA prototype. This then determined both the maximum dimensions and allowed volume for the electromagnetic hardware, and the amount of mass to be suspended. The stiffness required was determined from a calculation of the static stiffness of the existing air-bearings.

The structural modes of the supported structures were established using finite-element model analysis of the existing device. Since the linear motor on the translator head would be replicated, its velocity and acceleration profiles were specified. Finally, the maximum level of stray magnetic field both in the area of the recording head and near the disk were established from knowledge of the sensitivity of the magnetic domains in the recording material. The detailed specifications for the magnetic bearings are listed in Table 1.

Table 1. Specifications

Stiffness	
Parallel to disk	14 x 10^6 N/m
Normal to disk	9 x 10^6 N/m
Suspended mass	0.9 kilogram
Maximum force	18 newtons
Position Accuracy	2.5 microns
Bandwidth	100 hertz
Maximum dimensions	
Length	2.9 centimeter
Width	3.8 centimeter
Height	3.2 centimeter
Maximum acceleration	21 meters/sec^2
Maximum velocity	1.2 meters/sec
Maximum stray magnetic-field	
At read/write head	3 millitesla
At disk surface	0.2 tesla

2. MAGNETIC ACTUATORS

The prime objective of the translator bearing design was the definition of a magnetic-bearing alternative requiring minimal modifications of the existing system. The current system is shown in Figure 1. The read/write head is mounted in the aluminum carriage between the linear motors which are central to the whole assembly. Producing high forces, the linear motors use large samarium-cobalt magnets that create large magnetic fields in the air-gap (1.2 tesla). The shafts that carry the return flux are therefore large and double as air bearing surfaces. Actually, the air bearings are made by milling slots in the iron shaft and covering them with porous graphite. Air is then pumped into the slots and through the graphite, forming a cushion of air between the shaft and the aluminum carriage which it supports.

For an easy retrofit, the entire bearing and shaft structure cannot occupy more space than the current air bearing shaft. As such, the geometric constraints were the most restrictive. The tight spacing drove many of the design parameters and eliminated many configuration options. A second major restriction was imposed by magnetic flux of the linear motors. The twin voice-coil motors must move the read/write heads at high acceleration and, as such, require large magnetic flux density. This means that there must be a large pole-area facing the linear motor magnet (for uniform flux), and that the shaft must have sufficient cross sectional area to carry the return flux back to the motor magnet.

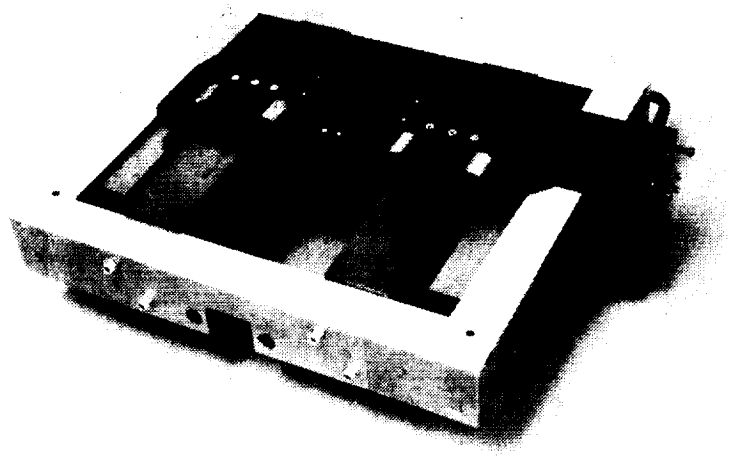

Figure 1. Present Air-Bearing System

uniform flux), and that the shaft must have sufficient cross sectional area to carry the return flux back to the motor magnet.

Together these restrictions quickly narrowed the actuator design options to that shown in Figure 2. Normally, a radially symmetrical four- or eight-pole design is used for magnetic bearings, but the linear-motor magnet flux prevented pole placement on one side. Fortunately, all five required degrees-of-freedom can be controlled with a three-pole design because the two bearing sets are mirror images of each other as shown in Figure 3, and can be coupled to provide the proper support. This configuration was chosen as the baseline because its layout is both simple mechanically and it has low internal flux-density. A permanent magnet is employed to provide bias flux. The bias flux is used because it provides a linear force-per-amp scale factor, and because it reduces power consumption for a given force capability. The complete magnetic design parameters are listed in Table 2.

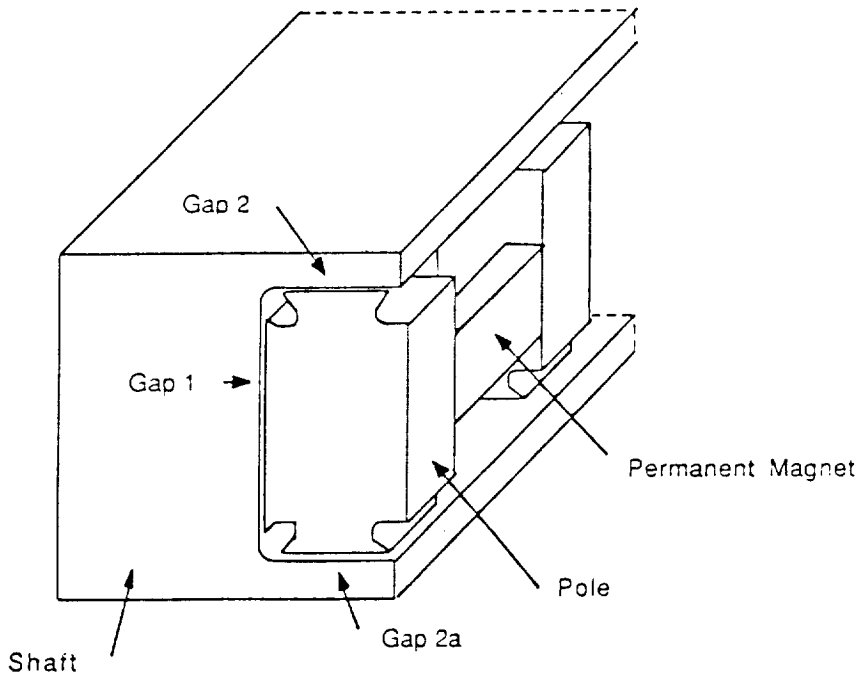

Figure 2. Actuator Design

Table 2. Design Parameters

X-Axis	
Unstable Frequency	45 Hz
Bias Field	0.149 T
Pole Area	3.78×10^{-4} m^2
Nominal Gap	2.54×10^{-4} m
Turns	130
Inductance	27 mHy
Wire Size	AWG32
Max Current (2g)	720 mA
Z-Axis	
Unstable Frequency	48 Hz
Bias Field	0.126 T
Pole Area	1.67×10^{-4} m^2
Nominal Gap	3.05×10^{-4} m
Turns	120
Inductance	21 mHy
Wire Size	AWG33
Max Current (2g)	580 mA
Magnet Parameters	
Material	SmCo
Energy Product	19 MGOe
Size	0.27cm x 0.45cm x 0.48 cm

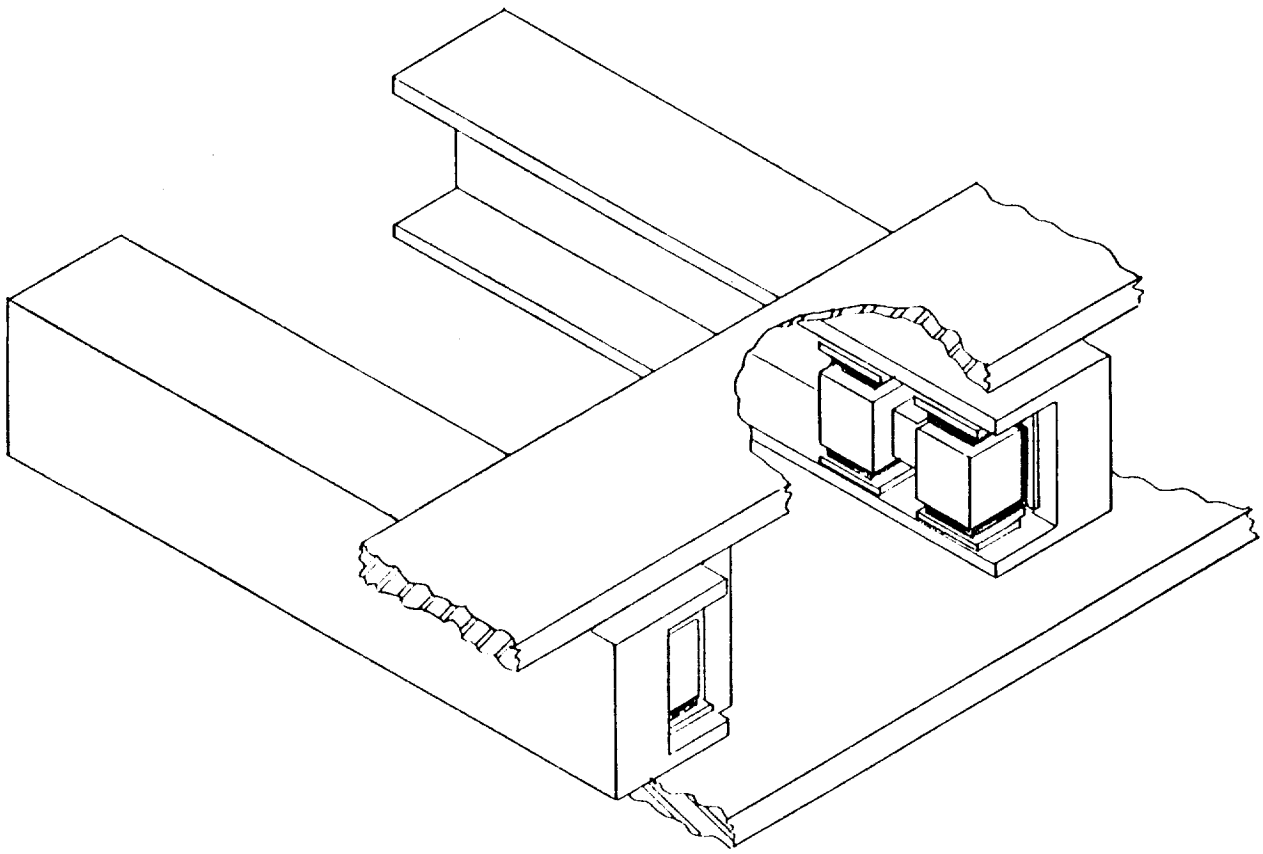

Figure 3. Magnetic Bearing System

3. START-UP/SHUT-DOWN PROCEDURE

A model was developed to simulate the collisions between bearing slide and frame in order to verify the stability characteristics of the bearing under very large disturbance conditions, and determine the transients occurring during startup and shutdown. Figure 4 shows the terminology and coordinate frame used in system modelling. The model is based in the following assumptions:

(1) All collisions are elastic, conserving both the total energy and linear/angular momentum,

(2) The frame mass M_f is much greater than slide mass M_s,

(3) The slide is assumed to be a thin, i.e its Z dimension or thickness is very small compared to the X dimension,

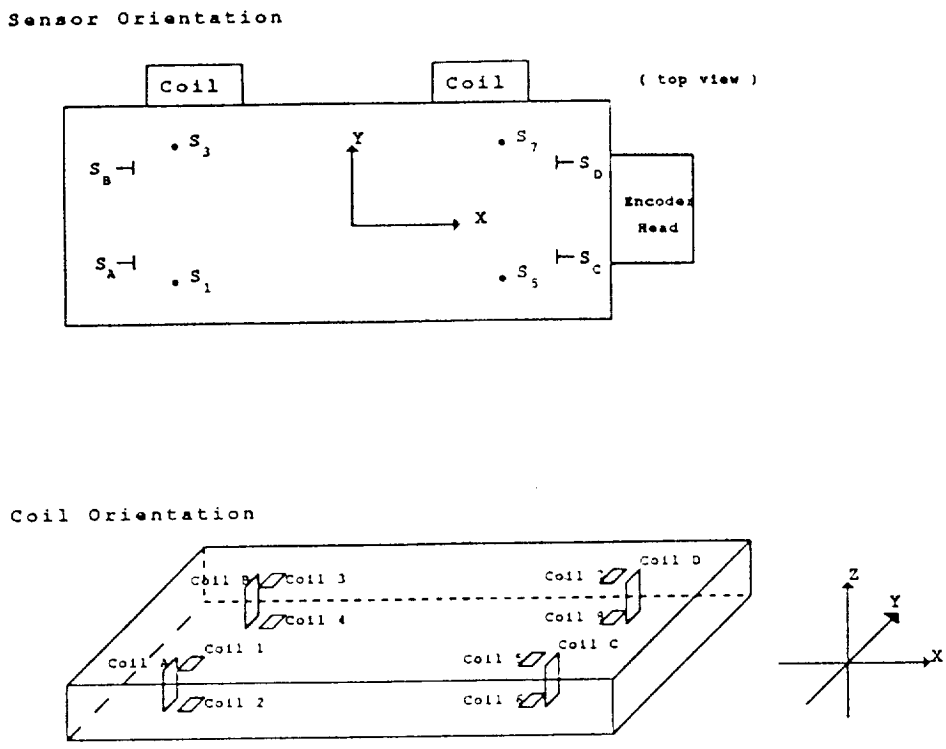

Figure 4. Terminology and Coordinate Frame

(4) Collisions are only along the X and Z axes, and are such that the collisions along the X axis occur only on the faces A, B, C or D, and collisions along the Z axis only at the corners 1 to 8 of Figure 3.

These assumptions imply that:

(a) a collision along the X axis will result in an instantaneous change in the X and Θ_z velocity components of the slide, and

(b) that a collision along the Z axis will result in an instantaneous change in the Z, Θ_x and Θ_y velocity components of the slide.

These equations are used in the nonlinear simulation to model collisions both during start-up and during large-scale transients. A start-up/shut-down strategy is considered necessary for the magnetic bearing to ensure smooth transition between the two extreme conditions of bearing parameter variation when the bearing slide is located in one corner of the frame as against the nominally centered operating condition. This procedure is complicated by the necessity to design the controller so that the bearing is insensitive to the direction of gravity when being tested under 1g conditions. The following assumptions were made to establish a start-up/shut-down strategy:

(1) No "gravity-direction" sensing allowed

(2) May start from the same corner each time

(3) The shut-down procedure brings the bearing to rest in the same corner every time

(4) The compensation may be changed when the bearing has passed from start-up to a nominally centered operating condition.

(5) Signal cross-coupling may be added to cancel the bearing cross-coupling terms when starting-up.

(6) The bearing may be started-up with suitable bias currents.

The start-up strategy adopted under the above assumptions is:

(a) Inject currents into the control coils such that start-up is from the corner $-\Delta x$, $-\Delta z$ which are the extreme possible displacements along the negative X and Z axes. Referring to Figure 3 this position is corner 2.

(b) Inject bias currents $I_{\beta ac}$, $I_{\beta bd}$, $I_{\beta 12}$, $I_{\beta 34}$, $I_{\beta 56}$, $I_{\beta 78}$ such that the actuators exert zero force on the bearing slide. The forces on the bearing are solely due to gravity.

(c) Command the control loops for regulating the X and Z displacements of the bearing slide with reference signals x_{ref} and z_{ref} which place it just slightly away from the start-up corner.

(d) Ramp the reference signals x_{ref} and z_{ref} down to zero at a rate slow enough assure dynamic stability of the regulation loops.

The resulting start-up waveforms are shown in Figure 5, where the bottom trace is the waveform used to command both the currents and the positions. The upper trace shows the start-up response of both the X and Z position signals.

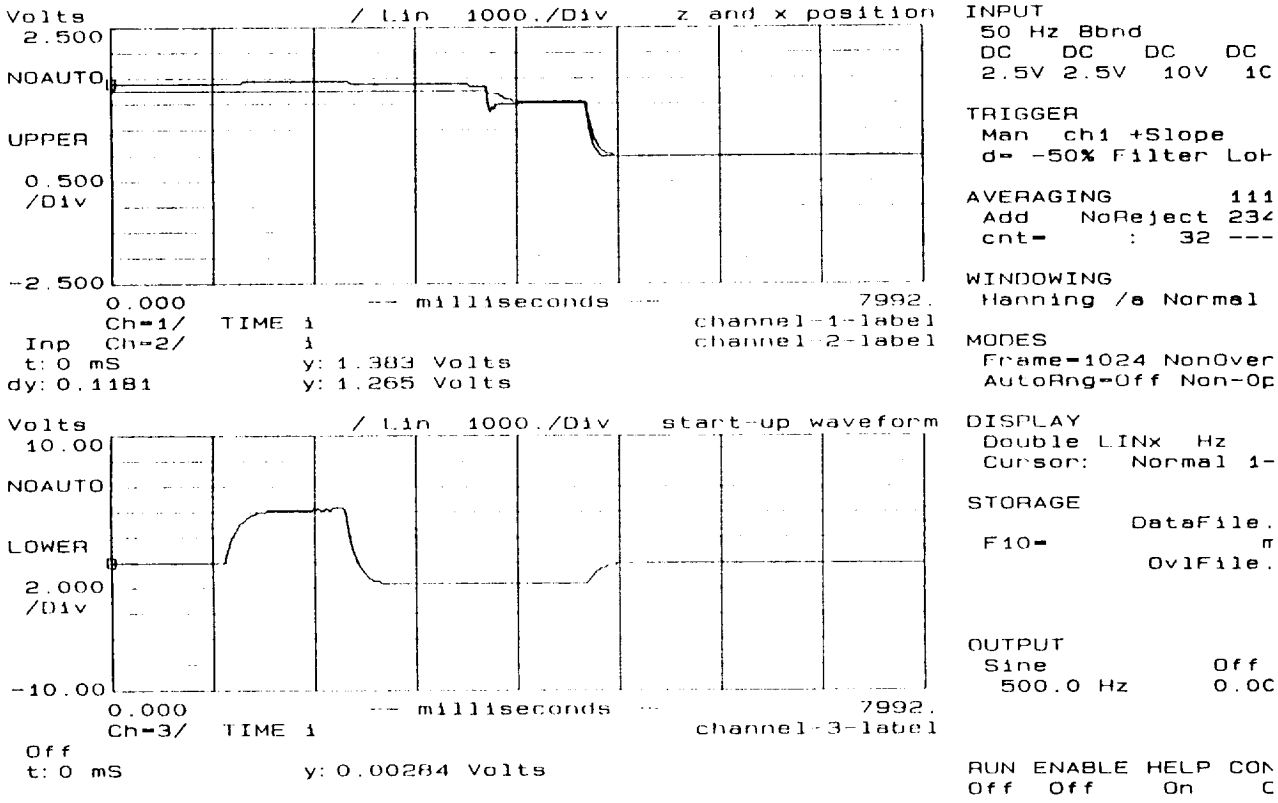

Figure 5. Start-Up Waveform

4. TEST RESULTS

The results of the static testing were good. The primary concerns were force gains, and eddy-current effects. A typical force versus current transfer function is shown in Figure 6. Though the force-per-amp gains are lower than expected, the system overdesign still allows production of the force levels required for 2g acceleration. The cross-coupling at the centered position is less than 2% X-current to Z-force, and less than 1% Z-current to X-force. At the worst case, one-half gap displacement in both X and Z, the cross coupling is only 12% X-current to Z-force, and 6% Z-current to X-force.

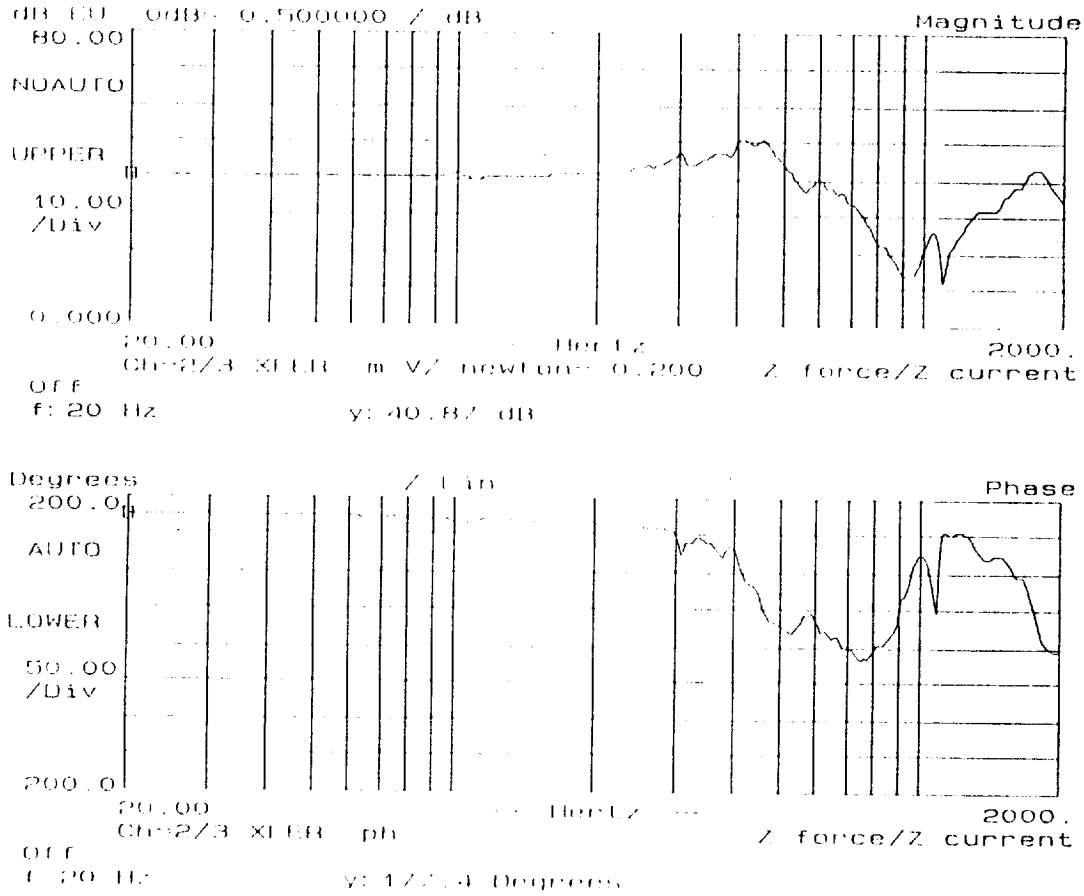

Figure 6. Force vs. Current Frequency Response

The eddy-current test results were also good. There were concerns that the force roll-off due to magnetic losses would limit the achievable bandwidth of the control loop. Fortunately, current to magnetic-field measurements, one of which is shown in Figure 7, indicate that the roll off is beyond 500 Hz with a phase loss of only 10° at 100 Hz.

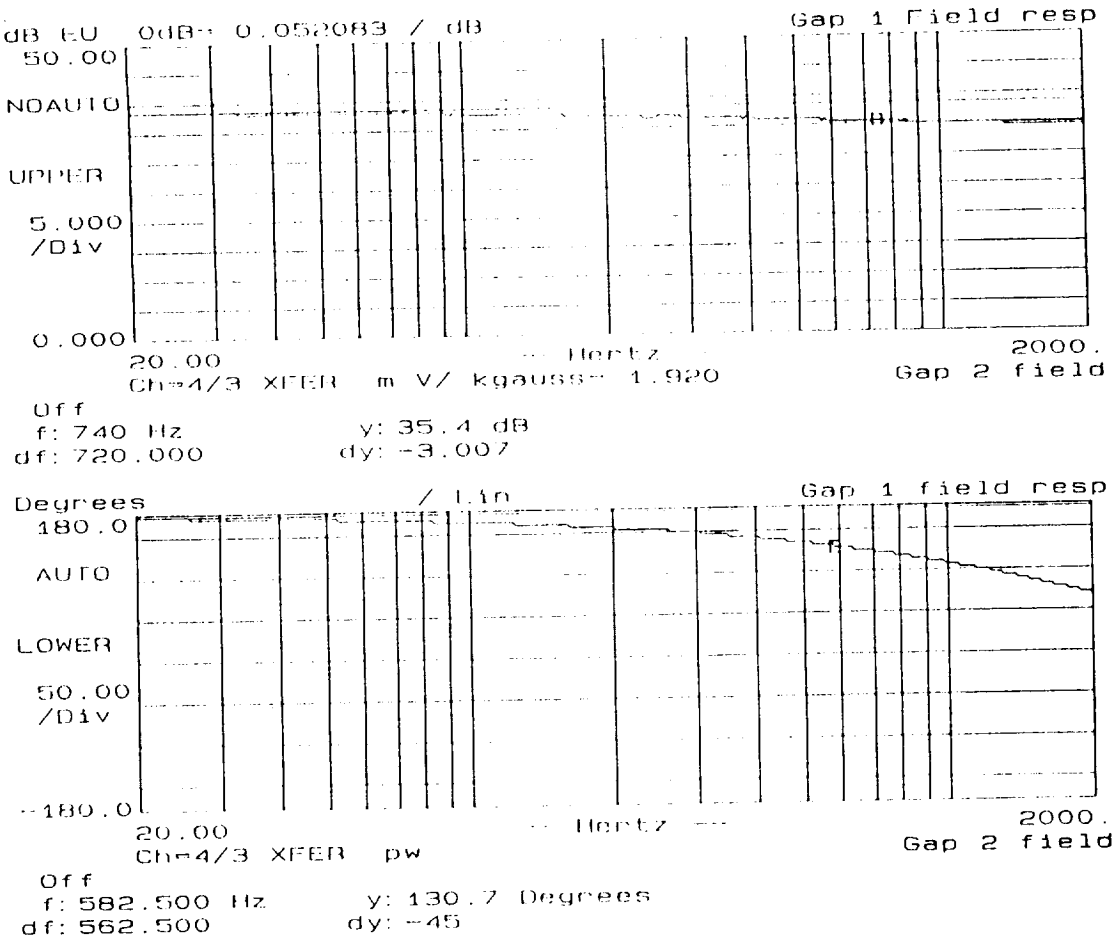

Figure 7. Flux vs. Current Frequency Response

Interaction between the linear-motor coils and the magnetic bearings was another area of concern. Preliminary analysis indicated that the disturbances should be small, but the geometry of the problem is too complicated for accurate analysis. The static test show the coupling gains to be less than 1 newton/amp below 100 Hz in the x-axis, and less than 0.5 newton/amp in the z-axis for excitation of one motor coil. Closed-loop testing consisted of frequency and step response measurements and disturbance sensitivity evaluation. A typical open-loop frequency response is shown in Figure 8. The loops were adjusted for gain crossover at 100 Hz, giving phase margins from 35 to 63 degrees. A typical step response is shown in Figure 9. The loops show little overshoot and good settling time.

The sensitivity of the magnetic bearing system to external disturbances was quantified in two ways: interaction with the linear motor, and bench-top "bang." Linear motor interaction was measured by the transfer function from linear motor current to both effort and motion in all five degrees-of-freedom. The θ_z loop had a significantly larger effort response than any other loop. This is due to the fact that both the sensors which measure θ_z, and the actuators which produce the torque about the Z axis had to be mounted along one of the short axes of the translator while the inertia about the θ_z axis is along the long axis. This mismatch results in a significantly reduced torque capability in the θ_z loop, and presents an interesting lesson for the design of future magnetic bearing systems.

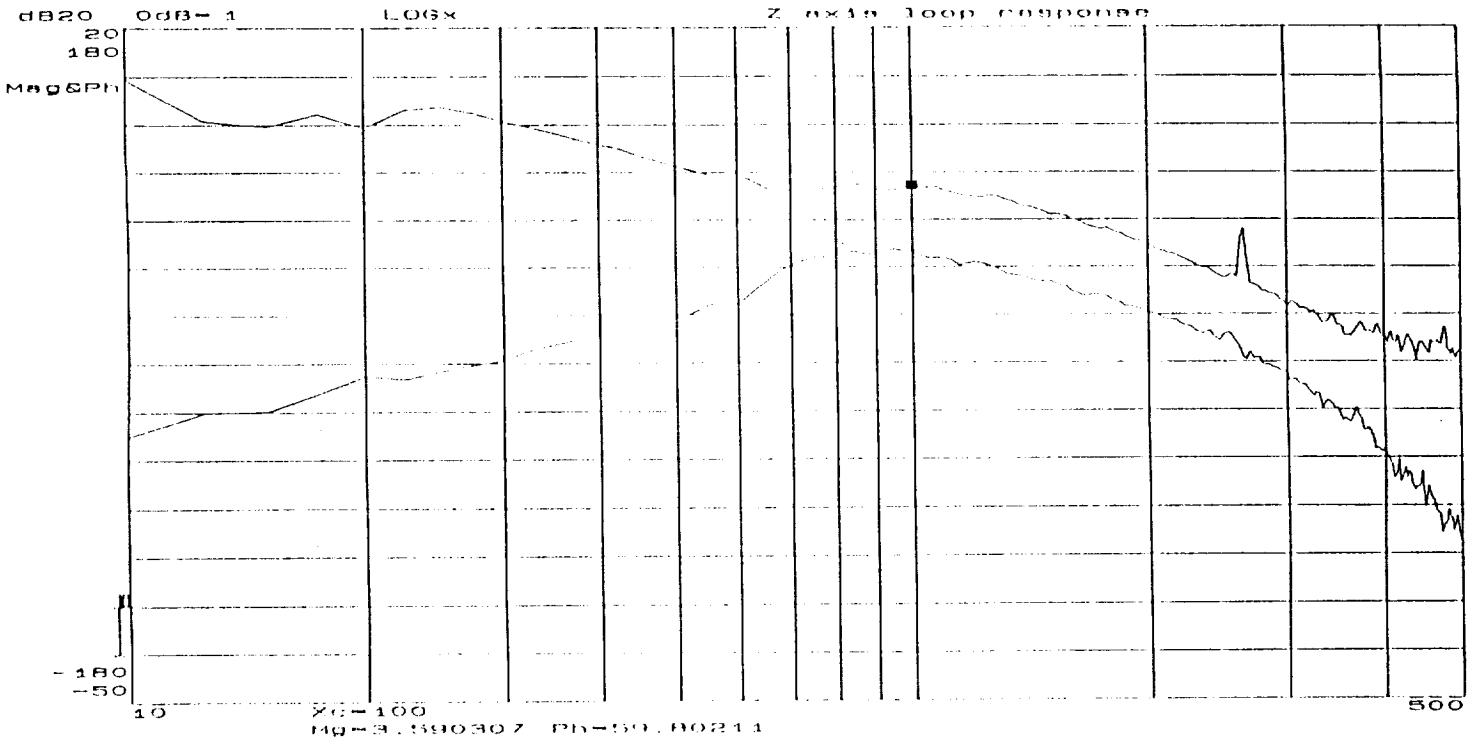

Figure 8. Open-Loop Frequency Response

The peak in the θ_z effort response occurs at about 95 Hz and is 18 volts/amp where saturation occurs at approximately 12 volts. The effort response does fall off rather quickly at both lower and higher frequencies, reaching 7 volts/amp at both 10 Hz and 200 Hz. The worst-case motion responses were 10 μ/amp in the Z loop and 0.2 mRad/amp in the θ_y loop.

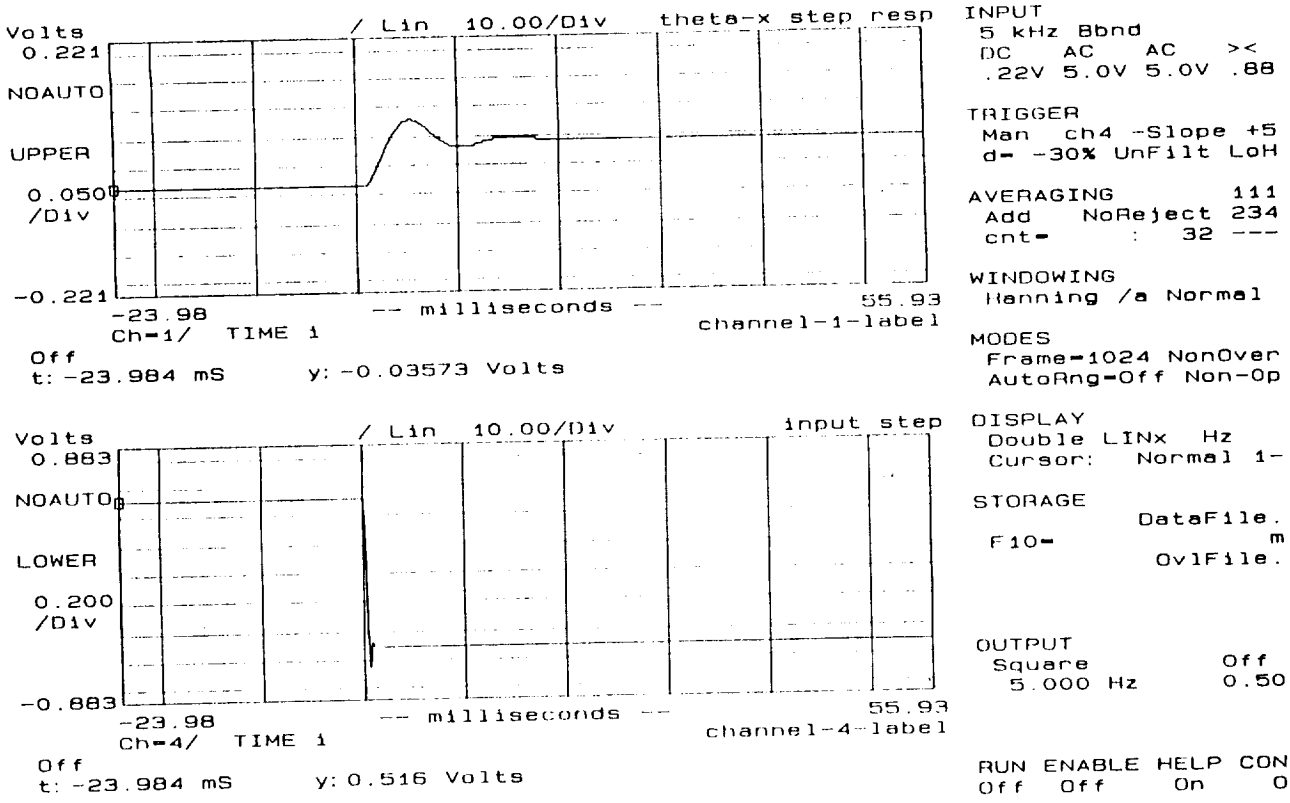

Figure 9. Step Response

A typical bench-top "bang" result is displayed by the displacement signals in the X and Z position loops in Figure 10. The range of the vertical axes on this plot represents the complete mechanical gap available for motion of the translator; thus, these plots show numerous collisions with the frame in the X axis. In all cases the loops recovered gracefully without significant overshoot.

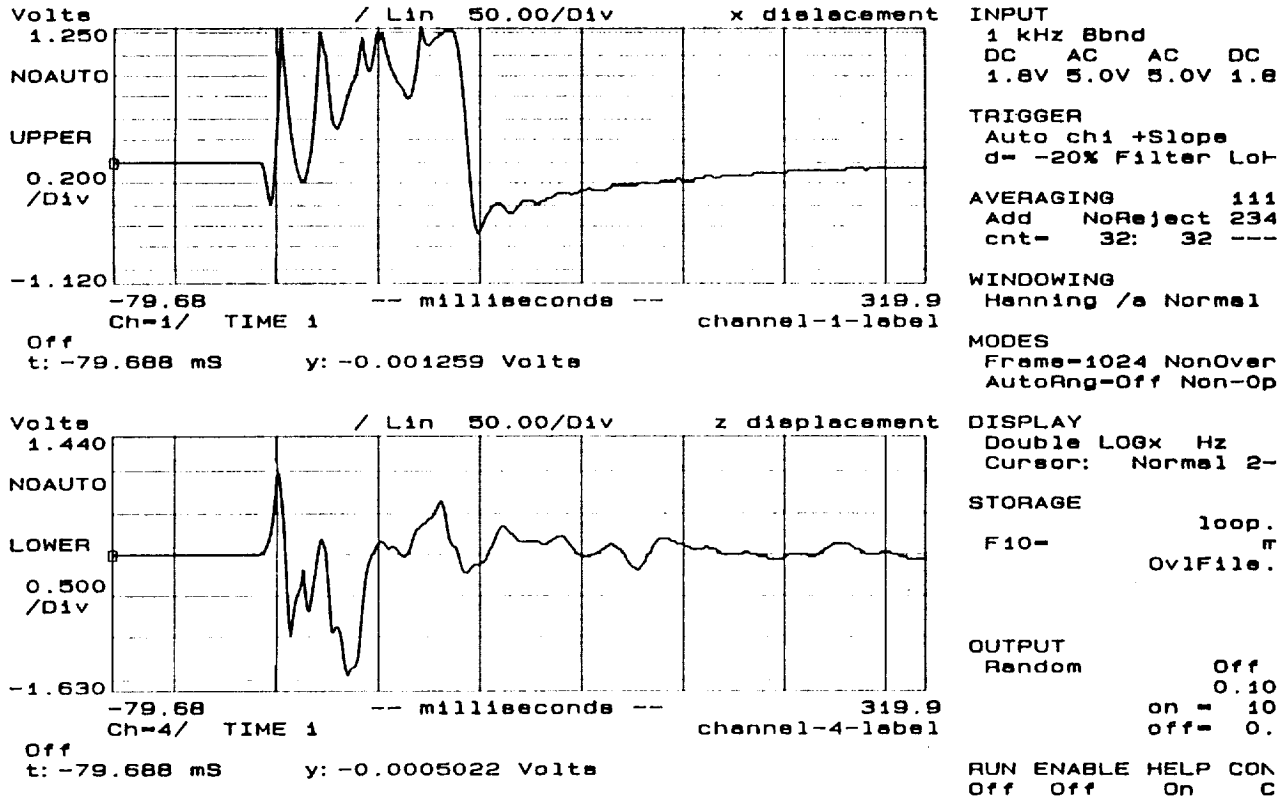

Figure 10. Bench-Top "Bang" Transient

5. CONCLUSIONS

The magnetic bearing control loops perform well, achieving 100 Hz nominal bandwidth with phase margins between 37 and 63 degrees. The lag in the actuator response from current to force produced by eddy-current losses introduces only 10 degrees of phase lag in the loop response at 100 Hz. The worst-case position resolution is 0.02 μ in the displacement loops and 1 μrad in the rotation loops. The system is very robust to shock disturbances, recovering smoothly even when collisions occur between the translator and frame. The start-up/shut-down circuit has proven very effective both in achieving initial levitation and in minimizing the "clunk" during turn-off.

The predominant shortcoming of the present system design is the gross mismatch between the center-of-mass of the translator and the center-of-effort of the magnetic actuators. This mismatch means that, in order to decouple the rotation loops from the displacement loops, some of the actuators must produce virtually no force. This restriction severely limits both the gain and the total force capability of the displacement loops. In addition, the large differences in actuator gains makes the process of adjusting the loop-decoupling very difficult. A system in which the center-of-mass was located close to the center-of-effort would be nearly inherently decoupled making any slight adjustment a trivial process. These effects should be considered in future system designs.

6. ACKNOWLEDGEMENTS

This work was performed for NASA, Goddard Space Flight Center under SBIR contract number NAS5-30309. The authors would like to acknowledge the guidance provided by John Sudey and Michael Hagopian of NASA.

7. REFERENCES

Downer, J.R., "Design of Large Angle Magnetic Suspensions," ScD Thesis, Massachusetts Institute of Technology, May 1986.

Hockney, R., and T. Hawkey, Magnetic Bearings for an Optical-Disk Buffer, SBIR Phase I Final Report. SatCon Technology Corp., R08-87, September 1987.

Roters, H., Electromagnetic Devices, New York: John Wiley & Sons, Inc., 1941.

Studer, P.A., Magnetic Bearings for Instruments in the Space Environment, NASA Technical Memorandum 78048, Goddard Space Flight Center, Greenbelt, Maryland, 1978.